Qinhui Wang*
Chengdong Ying
Ruiyue Zhang
Jianmeng Cen

Sulfur Transformation during Coal Pyrolysis with Char Heat Carrier

To investigate sulfur transformation during coal pyrolysis with char heat carrier (CHC), the effects of temperature, CHC/coal, and CHC production temperature were explored in a fluidized bed. The yield rates of sulfur in H_2S (Y_{H_2S}) and Y_{COS} elevated with temperature. Y_{CH_3SH} and $Y_{char\text{-}S}$ decreased, and temperature showed no significant effect on $Y_{tar\text{-}S}$. CHC inhibited sulfur transformation to the gas phase. More H_2S and COS were fixed in mixed-char in form of CaS by CHC, resulting in the increase of $Y_{char\text{-}S}$. CHC was favorable for CH_3SH decomposition. The inhibitory effect was enhanced with increasing CHC/coal. Higher production temperature inhibited the sulfur fixation capacity of CHC. CHC enhanced the decomposition of pyrite, organic sulfur, sulfate, and the yield of sulfide in mixed-char.

Keywords: Char heat carrier, Coal polygeneration, Coal pyrolysis, Sulfur transformation

Received: February 07, 2023; *revised:* March 23, 2023; *accepted:* May 25, 2023

DOI: 10.1002/ceat.202300091

Supporting Information available online

1 Introduction

According to the Statistical Review of World Energy 2022 by BP, China is the largest energy consumer in the world, accounting for 26.5 % of global primary energy consumption in 2021 [1]. Coal is the main energy source in China, and its utilization is relatively limited and inefficient, mainly for combustion and coal chemical industry.

Coal polygeneration technology is considered as a promising method for efficient utilization of coal. The heat of coal pyrolysis is provided by heat carrier in coal polygeneration technology. Volatile components are extracted from coal to obtain medium calorific value gas, tar, and char. The heat generated by the combustion of char is used for power generation and heat supply, so that heat, electricity, gas, and tar are produced in one system, achieving coal graded utilization and improving the coal utilization efficiency [2], as shown in Fig. S1 of the Supporting Information.

During this process, sulfur in coal will be exhausted to the atmosphere in the form of SO_X, causing environmental pollution [3]. Different from traditional coal pyrolysis technology, there is an interaction between CHC and coal, affecting the sulfur transformation. Therefore, it is of great significance to study the sulfur conversion process in coal pyrolysis polygeneration technology for pollution control.

Many researchers have investigated the effects of different factors on the sulfur transformation characteristics in traditional coal pyrolysis, such as temperature [4–6], pressure [7, 8], reaction time [9], atmosphere [10, 11], coal particle size [12, 13], heating rate [14, 15], and additives [16]. However, there are relatively few reports on sulfur conversion in coal polygeneration technology.

Char and combustion ash are commonly used as solid heat carriers in this technology. A few experimental investigations on sulfur transformation in coal pyrolysis with solid heat carriers have been conducted. Guo et al. [17] carried out coal pyrolysis experiments using recycled ash as heat carrier and found sulfur in char could be reduced to 70 % of sulfur in coal. Jia et al. [18] performed coal pyrolysis with different combustion ash/coal ratios, showing that ash inhibited H_2S release at low temperature but promoted H_2S release at high temperature, and more COS was released but the sulfur in tar was reduced. Pan et al. [19] used combustion ash and gasification char as heat carriers in coal pyrolysis and found 60–70 % of the sulfur in coal was fixed in heat carriers, and the sulfur fixation capacity of gasification char was stronger than ash. Fu et al. [20] conducted coal pyrolysis experiments using biomass char as heat carrier and found the nitrogen and sulfur in tar was reduced.

There are other factors affecting the sulfur transformation. Zhang et al. [21] investigated the interaction between coal pyrolysis volatiles and char, showing that more sulfur was transformed to gas below 600 °C, while more sulfur remained in char above 600 °C, and the distribution of sulfur forms on char surface was closely related to sulfur conversion. Meng et al. [22] investigated the effect of ash-ZnO complex on sulfur

Prof. Qinhui Wang (qhwang@zju.edu.cn), Chengdong Ying, Ruiyue Zhang, Jianmeng Cen
State Key Laboratory of Clean Energy Utilization, Institute for Thermal Power Engineering, Zhejiang University, Zheda Road, 310027 Hangzhou, China.

release during coal pyrolysis. Ash-ZnO inhibited the sulfur transformation to tar and gas.

In conclusion, there are few studies on sulfur conversion in pyrolysis coal using char heat carrier (CHC), and most studies only compare the differences between traditional pyrolysis and CHC pyrolysis. Hence, the mechanism of sulfur transformation is unclear. Besides, the changes of sulfur forms in mixed-char are rarely reported. In addition, the influencing factors investigated are not sufficient.

Therefore, an experimental study on the sulfur transformation of a typical coal in CHC pyrolysis process was carried out in a fluidized-bed reactor, and the effects of temperature, CHC production temperature, and CHC/coal on the sulfur content in gas, tar, and mixed-char were investigated. Meanwhile, the changes of sulfur forms in mixed-char were determined.

This work provides a reference for pollutant emission control in the utilization of coal pyrolysis polygeneration technology.

2 Experimental

2.1 Materials

A typical Chinese coal, Xin Jiang Run Bei coal (XJRB), was used in the study. The heat carrier was XJRB char, the preparation of which is as follows: 30 g XJRB was placed in the fluidized-bed reactor for a 30-min pyrolysis in Ar atmosphere, and the temperatures were 850 °C, 880 °C and 900 °C. The CHCs obtained at different temperatures were denoted as 850 °C-CHC, 880 °C-CHC, and 900 °C-CHC, respectively.

XJRB and CHCs were sieved to 0.9–2.5 mm, of which the ultimate and proximate analysis results are listed in Tab. 1. XJRB and CHCs were dried at 105 °C for 24 h to remove moisture. The sulfur forms in XJRB and CHCs are presented in Tab. 2.

2.2 Apparatus and Procedure

2.2.1 Apparatus

The experiments were carried out in a fluidized bed, as displayed in Fig. S2, consisting of furnace, gas system, screw feeder, cyclone separator, tar collection unit, gas collection unit, and distributed control system (DCS).

Table 2. Sulfur forms in XJRB and CHCs.

Sample, ad [wt%]	S_T [a]	S_s [b]	S_p [c]	S_o [d]	$S_{sulfide}$ [e]
XJRB	2.43	0.24	0.76	1.43	0.00
850 °C-CHC	2.24	0.00	0.04	1.10	1.10
880 °C-CHC	2.23	0.00	0.04	1.14	1.05
900 °C-CHC	2.21	0.00	0.04	1.01	1.16

[a] Total sulfur; [b] pyrite; [c] sulfate; [d] organic sulfur; [e] by difference.

2.2.2 Procedure

The experimental procedure is illustrated in the Supporting Information. A series of experiments were carried out, as indicated in Tab. 3. Groups 1–3 were set to study the effects of pyrolysis temperature and CHC/coal and groups 4–6 to examine the effect of CHC production temperature.

Table 3. Operating parameters for different conditions.

Group	CHC	CHC/coal	Temp. [°C]	Atmosphere
1	850 °C-CHC	0	600, 650, 700, 750	Ar
2		3		
3		5		
4	850 °C-CHC	3	600, 650, 700, 750	Ar
5	880 °C-CHC			
6	900 °C-CHC			

2.3 Analysis

There were three pyrolysis products, namely, gas, tar, and mixed-char. The composition of gas and the concentration of sulfur-containing gases were analyzed in a gas chromatograph (GC, Agilent 7890A) equipped with a flame photometric detector (FPD). The sulfur content of tar was analyzed in a fluores-

Table 1. Ultimate and proximate analysis of XJRB and CHCs.

Samples	Proximate analysis, ad [wt %]				Ultimate analysis, ad [wt %]				
	M [a]	A [b]	V [c]	FC [d]	C	H	N	O [e]	S
XJRB	1.23	11.09	38.66	49.02	67.19	4.16	1.21	12.68	2.43
850 °C-CHC	2.29	19.92	5.65	72.14	72.33	1.05	1.12	1.47	2.24
880 °C-CHC	1.84	16.76	4.97	76.43	75.89	1.24	1.26	0.78	2.23
900 °C-CHC	2.54	19.68	4.52	73.26	73.12	1.18	1.19	0.08	2.21

[a] Moisture; [b] ash; [c] volatile; [d] fixed carbon; [e] oxygen, O = 100 – M – A – C – H – N – S.

cent sulfur analyzer (KY-3000SN, Jiangsu Keyuan). A Kulun sulfur tester (CLS-2, Jiang Fen) was employed to determine the sulfur content in mixed-char. A 2°/min scanning-rate Panalytical X'Pert'3 Powder XRD system using AlKα ($h\nu$ = 1486.6 eV) X-ray source was adopted for characterizing the crystalline phases of the mixed-char and CHCs. The sulfur forms in XJRB, CHCs, and mixed-chars were determined according to the Chinese Standard GB/T 215-2003 and a previous work [23].

All calculations were performed according to the following equations[1)]:

$$V_{gas} = \frac{V_{Ar}}{C_{Ar}} \quad (1)$$

$$Y_{H_2S/COS/CH_3SH} = \frac{C_{H_2S/COS/CH_3SH} V_{gas} \times 32/V_m}{M_{coal} S_T} \times 100\% \quad (2)$$

$$Y_{tar\text{-}S} = \frac{M_{tar} S_{tar}}{M_{coal} S_T} \times 100\% \quad (3)$$

$$Y_{char\text{-}S} = \frac{M_{char} S_{char} - M_{CHC} S_T}{M_{coal} S_T} \times 100\% \quad (4)$$

$$D_i = \frac{S_{i\text{-}char} M_{char} - S_{i\text{-}CHC} M_{CHC}}{S_{i\text{-}coal} M_{coal}} \times 100\% \quad (5)$$

As shown in Tab. 2, there was no sulfide detected in raw coal and therefore the total sulfur mass in coal sample was used as denominator to calculate the $Y_{sulfide}$.

$$Y_{sulfide} = \frac{S_{sulfide\text{-}char} M_{char} - S_{sulfide\text{-}CHC} M_{CHC}}{S_T M_{coal}} \times 100\% \quad (6)$$

V_{gas} (L) is the total gas volume; V_{Ar} (L) is the Ar volume consumed in 6 min; C_{ar} (vol %) is the Ar concentration in gas; $Y_{H_2S/COS/CH_3SH}$ (wt %) denotes the yield rates of sulfur in H_2S, COS, or CH_3SH, respectively; $C_{H_2S/COS/CH_3SH}$ (vol %) are the concentrations of H_2S, COS, or CH_3SH, respectively; V_m (L mol^{-1}) is the molar volume of gas; M_{coal} (g) is the sample weight; S_T (wt %) is the total sulfur content; $Y_{tar\text{-}S}/Y_{char\text{-}S}$ (wt %) are the yield rates of sulfur in tar or mixed-char, respectively; $M_{tar}/M_{char}/M_{CHC}$ (g) are the mass of tar, mixed-char, or CHC, respectively; S_{tar}/S_{char} (wt %) are the sulfur contents in tar or mixed-char, respectively; D_i (wt %) denotes the decomposition rates of sulfur in i, where i represents one of sulfate, pyrite, and organic sulfur; $S_{i\text{-}char}/S_{i\text{-}CHC}/S_{i\text{-}coal}$ (wt %) are the sulfur contents of i in mixed-char, CHC, or coal, respectively; $Y_{sulfide}$ (wt %) is the yield rate of sulfur in sulfide; $S_{sulfide\text{-}char}/S_{sulfide\text{-}CHC}$ (wt %) are the sulfur contents of sulfide in mixed-char or CHC, respectively.

1) List of symbols at the end of the paper.

2.4 Pre-Test

2.4.1 Mass Balance of Sulfur

To ensure the reliability of this experiment, a pre-test (without CHC) was conducted to check the mass balance of sulfur; results are presented in Tab. 4. The mass balance of sulfur was between 91.47 and 94.63 %, which was acceptable. The experimental error was attributed to three aspects: (i) gas, tar, and mixed-char could not be completely collected; (ii) some sulfur-containing gases with low concentration, C_2H_5SH, etc., were not analyzed in this study; (iii) there were errors in the analysis process of sulfur content in gas, tar, and mixed-char.

Table 4. Mass balance of sulfur during coal pyrolysis in the fluidized-bed reactor.

Temp. [°C]	Y_{H_2S} [wt %]	Y_{COS} [wt %]	Y_{CH_3SH} [wt %]	$Y_{tar\text{-}S}$ [wt %]	$Y_{char\text{-}S}$ [wt %]	Total [wt %]
600	26.80	3.60	2.46	2.78	56.48	92.12
650	30.65	4.10	2.18	2.85	51.69	91.47
700	33.86	4.79	2.00	2.87	51.11	94.63
750	34.61	4.90	1.58	2.76	48.29	92.14

2.4.2 XRD Analysis of CHCs

For a better study of the effect of CHC on sulfur transformation later, X-ray diffraction (XRD) analysis of the CHCs was carried out. There were various minerals in the CHCs, SiO_2, NaCl, FeS, CaS, CaO, and $Ca(OH)_2$, but barely no $CaSO_4$ and FeS_2 existed as displayed in Fig. S3, because $CaSO_4$ and FeS_2 were almost decomposed completely above 850 °C through the following reactions [24]:

$$4H_2 + CaSO_4 \rightarrow CaO + 3H_2O + H_2S \quad (7)$$

$$4H_2 + CaSO_4 \rightarrow CaS + 4H_2O \quad (8)$$

$$H_2 + CaSO_4 \rightarrow CaO + H_2O + SO_2 \quad (9)$$

$$4CO + CaSO_4 \rightarrow CaS + 4CO_2 \quad (10)$$

$$CO + CaSO_4 \rightarrow CaO + CO_2 + SO_2 \quad (11)$$

$$2C + CaSO_4 \rightarrow CaS + 2CO_2 \quad (12)$$

$$C + 2CaSO_4 \rightarrow 2CaO + 2SO_2 + CO_2 \quad (13)$$

$$2C + CaSO_4 \rightarrow CaO + CO_2 + COS \quad (14)$$

$$FeS_2 \rightarrow FeS + \frac{1}{n} S_n \quad (15)$$

$$FeS_2 + H_2 \rightarrow FeS + H_2S \quad (16)$$

$$FeS + H_2 \rightarrow Fe + H_2S \quad (17)$$

$Ca(OH)_2$ was formed through the water absorption of CaO.

3 Results and Discussion

3.1 Effects of Temperature and CHC/Coal

3.1.1 Effects of Temperature and CHC/Coal on Gaseous Sulfur

In this experiment, only three sulfur-containing gases, H_2S, COS, and CH_3SH, were detected in the gas products, and their yields were depicted in Fig. 1. All the statistics are normalized based on the sulfur content in ultimate analysis. Y_{H_2S} elevated gradually from 26.8^% to 34.61^% when the pyrolysis temperature increased from 600^°C to 750 °C in the absence of CHC. Moreover, the increment of Y_{H_2S} was more obvious at lower temperatures (< 700 °C), which was mainly attributed to the decomposition of pyrite and unstable organic sulfur in coal.

The increase in Y_{H_2S} became smaller at high temperatures (> 700 °C), which was due to two reasons: (i) as mentioned above, most of the easily decomposable sulfur had been decomposed below 700 °C, so that there was less H_2S released above 700 °C; (ii) more H_2S was captured by the alkaline minerals in coal at higher temperatures [25, 26]. To verify this, XRD analysis of the mixed-chars after pyrolysis was performed, as can be seen in Fig. S4. CaO was the main component with sulfur fixation ability among those alkaline minerals. The signal of CaS was enhanced as the temperature increased, indicating that more H_2S was fixed during pyrolysis by Eq. (18).

$$CaO + H_2S \rightarrow CaS + H_2O \quad (18)$$

Chauk et al. [27] also found that the sulfur fixation rate of CaO elevated from 20 % to nearly 100 % under 1 MPa when the pyrolysis temperature increased from 650 °C to 900 °C.

Compared with the groups without CHC, when CHC/coal was 3, Y_{H_2S} reduced by 1.72 % and 3.94 % at 600 °C and 700 °C, respectively. As CHC/coal rises, more CaO is introduced into the reactor, thus capturing more H_2S.

The Y_{COS} at different temperatures and CHC/coal is presented in Fig. 1b. During the pyrolysis process, COS was mainly generated through the following pathways: (i) reactions between the elemental sulfur from the decomposition of pyrite as well as pyrite itself and CO produced in pyrolysis; (ii) decomposition of organic sulfur; (iii) secondary reactions of H_2S with CO or CO_2 [28].

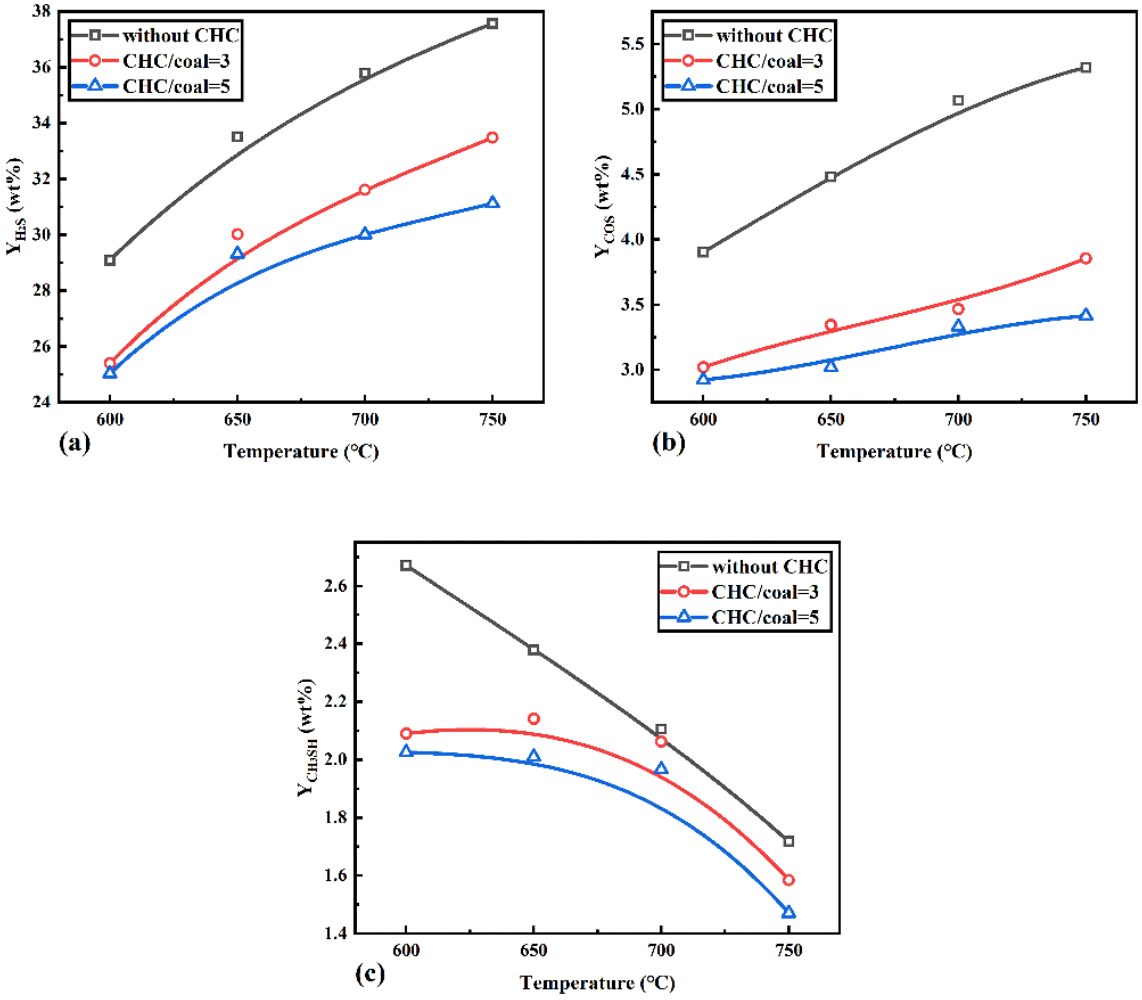

Figure 1. Yield rates of gaseous sulfur at different temperatures and CHC/coal: (a) Y_{H_2S}; (b) Y_{COS}; (c) Y_{CH_3SH}.

$$FeS + CO \rightarrow FeS + COS \quad (19)$$

$$S_n + nCO \rightarrow nCOS \quad (20)$$

$$H_2S + CO \rightarrow COS + H_2 \quad (21)$$

$$H_2S + CO_2 \rightarrow COS + H_2O \quad (22)$$

As can be seen, the increase of temperature could promote Y_{COS}. CHC could significantly inhibit the Y_{COS}, and this inhibitory effect was slightly enhanced with the increase of CHC/coal, which was due to the COS fixation ability of CaO in CHC [29].

$$CaO + COS \rightarrow CaS + CO_2 \quad (23)$$

Fig. 1c shows the variation of Y_{CH_3SH} with temperature and CHC/coal. The decomposition of organic sulfur during pyrolysis was the main source of CH_3SH [30]. Y_{CH_3SH} was relatively low, about 2 %, and decreased gradually with the rise of both temperature and CHC/coal. CH_3SH decomposes at high temperatures through the following reactions, which are endothermic, promoted by the increasing temperature, and therefore Y_{CH_3SH} decreased:

$$CH_3SH \rightarrow CH_3S + H \quad \Delta H = 385 \text{ kJ mol}^{-1} \quad (24)$$

$$CH_3SH \rightarrow CH_3 + SH \quad \Delta H = 322 \text{ kJ mol}^{-1} \quad (25)$$

CHC could reduce Y_{CH_3SH}, which was mainly attributed to the catalytic effect of the minerals in CHC.

3.1.2 Effects of Temperature and CHC/Coal on $Y_{tar\text{-}S}$ and $Y_{char\text{-}S}$

The effects of temperature and CHC/coal on $Y_{tar\text{-}S}$ are presented in Fig. 2a. $Y_{tar\text{-}S}$ was mainly generated through: (i) the decomposition of organic sulfur; (ii) the combination of organic groups with HS·. $Y_{tar\text{-}S}$ was around 3 %, and there was no significant change with the increase of temperature. $Y_{tar\text{-}S}$ was reduced to about 2 % with the addition of CHC, and it decreased with the increase of CHC/coal. This was mainly due to the presence of CaO and $Fe_{1-x}S$ in CHC, which could enhance the decomposition of organic sulfur in tar [31]. Attar [32] found that $Fe_{1-x}S$ had a catalytic effect on the desulfurization of organic sulfur, resulting in the reduction of $Y_{tar\text{-}S}$. In addition, HS· and the sulfur from the decomposition of aryl sulfides and mercaptans were combined with CaO from CHC, the $Y_{tar\text{-}S}$ was inhibited therefore [29].

Fig. 2b shows the changes of $Y_{char\text{-}S}$ with temperature and CHC/coal. $Y_{char\text{-}S}$ gradually decreased as the temperature increased due to the conversion of more sulfur in raw coal into gas and tar. Compared with groups without CHC addition, $Y_{char\text{-}S}$ elevated significantly with CHC, and the enhancement increased with higher CHC/coal. This can be explained in two aspects. On the one hand, H_2S and COS were captured by CaO in CHC to form CaS residue in mixed-char; on the other hand, there were a large number of microporous structures in the surface of 850 °C-CHC (Fig. S5), which could adsorb some gaseous sulfur. In addition, Setywati et al. [33] found that inorganic substances, like sodium chloride, could react with sulfur during pyrolysis to fix sulfur in mixed-char. According to the XRD analysis of CHC (Fig. S3), there was NaCl in CHC.

3.2 Effects of CHC Production Temperature

3.2.1 Effect of CHC Production Temperature on Gaseous Sulfur

The Y_{H_2S}, Y_{COS}, and Y_{CH_3SH} with three CHCs (850 °C-CHC, 880 °C-CHC, and 900 °C-CHC) at different temperatures are displayed in Fig. 3.

The effects of three CHCs on Y_{H_2S} showed the same trend, and all of them could inhibit the release of H_2S during pyrolysis. However, the inhibition effect was influenced by the CHC production temperatures. As demonstrated in Fig. 3a, with the CHC production temperature increasing from 850 °C to 900 °C, the Y_{H_2S} decreased by 3.1 %, 2.64 %, and 2.09 % at

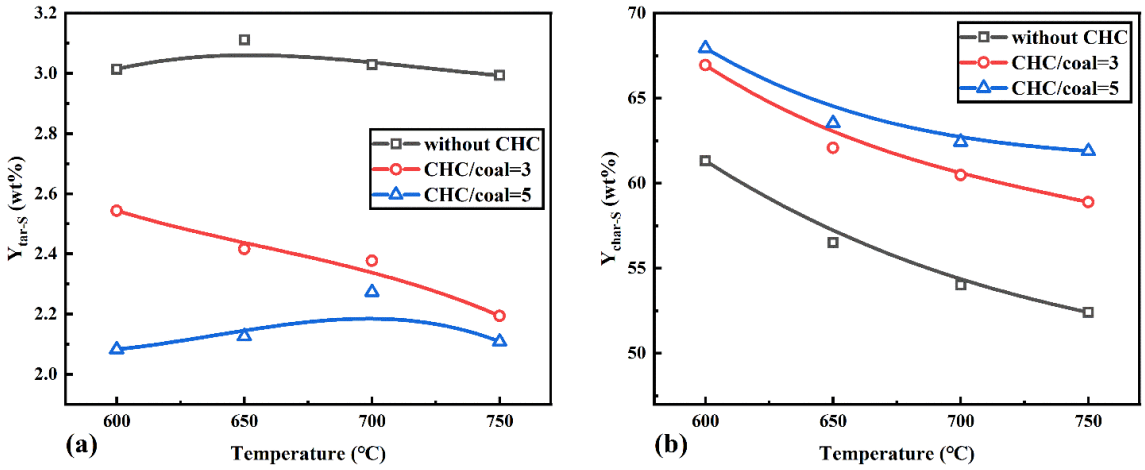

Figure 2. Effect of CHC/coal on (a) $Y_{tar\text{-}S}$; (b) $Y_{char\text{-}S}$.

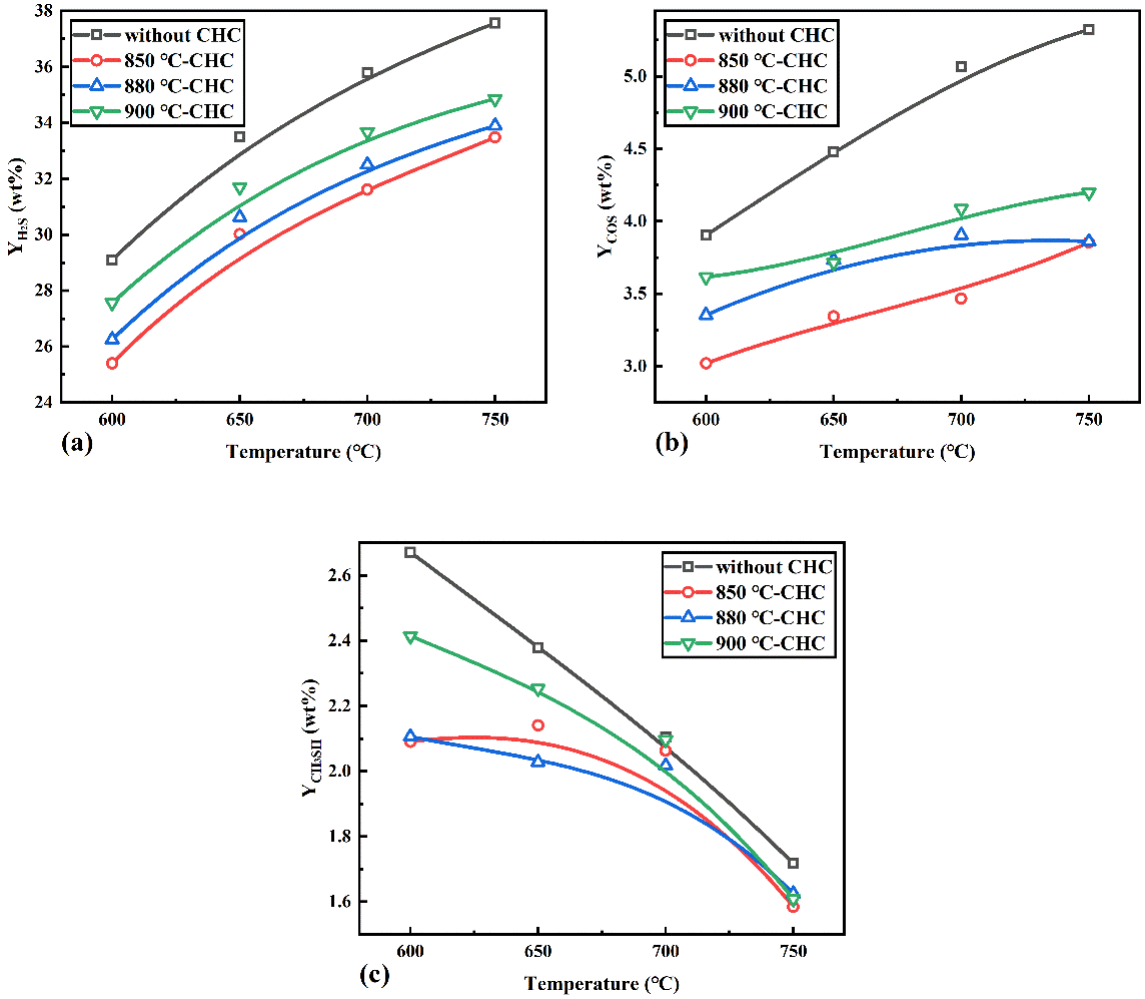

Figure 3. Effect of CHC production temperature on gaseous sulfur: (a) Y_{H_2S}; (b) Y_{COS}; (c) Y_{CH_3SH}.

750 °C, respectively, suggesting that the inhibition effect on gaseous sulfur generation of the three CHCs was ranked as follows: 850 °C-CHC > 880 °C-CHC > 900 °C-CHC.

To further study the mechanism, N_2 adsorption-desorption experiments and scanning electron microscopy (SEM) were conducted to obtain more information about the porous texture of the CHCs, as indicated in Tab. 5 and Fig. S5, respectively.

The raw coal sample exhibited an initial specific surface area of 0.41 m^2g^{-1}. After pyrolysis for 30 min, 850 °C-CHC had the largest surface area of 0.83 m^2g^{-1} among these three CHCs.

Table 5. Surface area of raw coal and CHCs.

Sample	Surface area [m^2g^{-1}]
XJRB	0.41
850 °C-CHC	0.83
880 °C-CHC	0.45
900 °C-CHC	0.18

During the pyrolysis process, the volatile components in raw coal were released, resulting in a large number of microporous structures in the CHCs, and the surface area of CHC increased. As the CHC production temperature was further raised to 900 °C, the surface area of CHC decreased to 0.18 m^2g^{-1}. This was because when the temperature was too high, the microporous structures started to be sinter [34]. The SEM images of CHCs were used to verify this. As can be seen in Fig. S5, the number of microporous structures in the three CHCs were ranked as follows: 850 °C-CHC > 880 °C-CHC > 900 °C-CHC, which was the same order as sorting by surface area.

The mutual reaction between CHC and pyrolysis gas was hindered by the decrease in microporous structures, and therefore the inhibition effect on the Y_{H_2S} of 900 °C-CHC was the weakest. In addition, Zhao et al. [35] found that the desulfurization capacity of CaO gradually decreased when the temperature was higher than 850 °C. This was attributed to the reduction of surface area caused by the sintering phenomena of CaO, which hindered the reaction between CaO and gaseous sulfur. It was corresponding to the presented results above.

The effects of three CHCs on Y_{COS} were almost the same as that on Y_{H_2S}, as shown in Fig. 3b. 850 °C-CHC, 880 °C-CHC,

and 900 °C-CHC could all reduce the Y_{CH_3SH} slightly, but the CHC production temperature showed no significant effect on Y_{CH_3SH}, which was due to the relatively low Y_{CH_3SH} in this experiment.

3.2.2 Effect of CHC Production Temperature on $Y_{tar\text{-}S}$ and $Y_{char\text{-}S}$

Fig. 4a presents the effect of CHC production temperature on $Y_{tar\text{-}S}$. All three CHCs could reduce the $Y_{tar\text{-}S}$, but $Y_{tar\text{-}S}$ showed a rising trend with the increase of CHC production temperature. The higher the temperature was, the more severe the CHC sintering level became, which weakened the interaction between CHC and tar, and therefore the facilitating effect of CaO and $Fe_{1-x}S$ in CHC on the decomposition of organic sulfur in tar was weakened.

Fig. 4b demonstrates the effect of CHC production temperature on $Y_{char\text{-}S}$. All three CHCs could promote $Y_{char\text{-}S}$, and $Y_{char\text{-}S}$ showed a decreasing trend with the rise of CHC production temperature. As mentioned above in Sect. 3.2.1, the desulfurization capacity of CHC was decreased when the production temperature was elevated, so more sulfur was transformed into gas and tar, and less sulfur was residue in mixed-char.

3.3 Variation of Sulfur Forms During Pyrolysis

The variations of D_{pyrite}, $D_{organic}$, $D_{sulfate}$, and $Y_{sulfide}$ during pyrolysis with temperature are illustrated in Fig. 5. Experiments without CHC were set as the blank control groups to investigate the effect of CHC on sulfur forms. According to the results above, 850 °C-CHC exhibited the best sulfur-fixation performance, so it was chosen to be the CHC of the experimental groups and the CHC/coal was 3.

Fig. 5a depicts the variation of D_{pyrite}, gradually elevating as the temperature increased. At 750 °C, the D_{pyrite} was close to 100 %, suggesting that the pyrite was almost decomposed completely. In addition, 850°C-CHC could facilitate the D_{pyrite} in the range of 600 °C–750 °C.

Fig. 5b shows the variation of $D_{organic}$, ranging from 55 % to 70 %. As the pyrolysis temperature increased, $D_{organic}$ firstly decreased to a minimum at 700 °C, which was attributed to two reasons. Firstly, D_{pyrite} increased at the same time, leading to an increment in gaseous sulfur and more sulfur was captured by the organic groups in coal to form new organic sulfur. Thus, $D_{organic}$ declined. But the effect of this reason should not have caused so much reduction in $D_{organic}$, so secondly, the increasing temperature caused the organic groups to condense and become less likely to release sulfur, resulting in a lower $D_{organic}$. Then $D_{organic}$ rose over 700 °C because those condensed groups were broken. Compared with no addition of CHC, 850 °C-CHC was able to promote the $D_{organic}$, which was attributed to the CaO in CHC, reacting with H_2S and COS to inhibit the conversion of gaseous sulfur to organic sulfur. This promotion effect became stronger with increasing temperature. When the temperature was higher than 700 °C, $D_{organic}$ was enhanced significantly with CHC. This was related to the reaction between carbon in coal and sulfate, which was enhanced by CHC. As a result, more C was consumed, and more chemical bodings between C and S were broken, more organic sulfur was released to take part in the pyrolysis process, leading to a higher $D_{organic}$.

Fig. 5c shows the variation of $D_{sulfate}$. At 600 °C, only about 10 % of sulfate was decomposed because it was considered to be difficult for $CaSO_4$ to decompose at this temperature, but easy for the decomposition of $FeSO_4$ and $Fe_2(SO_4)_3$. $D_{sulfate}$ increased with the temperature. At 750 °C, it reached 65.9 %, indicating that a higher temperature effectively promoted the $D_{sulfate}$. In addition, $D_{sulfate}$ was also enhanced by 850 °C-CHC, because CHC had a catalytic effect on the $D_{sulfate}$ as well as on the carbon reduction reaction of $CaSO_4$ (Eqs. (12)–(14)). By determining the carbon content of the mixed-chars, as indicated in Tab. 6, this assumption can be verified. The carbon content in the mixed-char produced with 850 °C-CHC was lower.

Fig. 5d shows the variation of $Y_{sulfide}$ (mainly CaS and FeS), promoted with the increasing temperature and the 850 °C-CHC addition, which could be explained by the following two aspects: firstly, the CaO in CHC could fix H_2S and

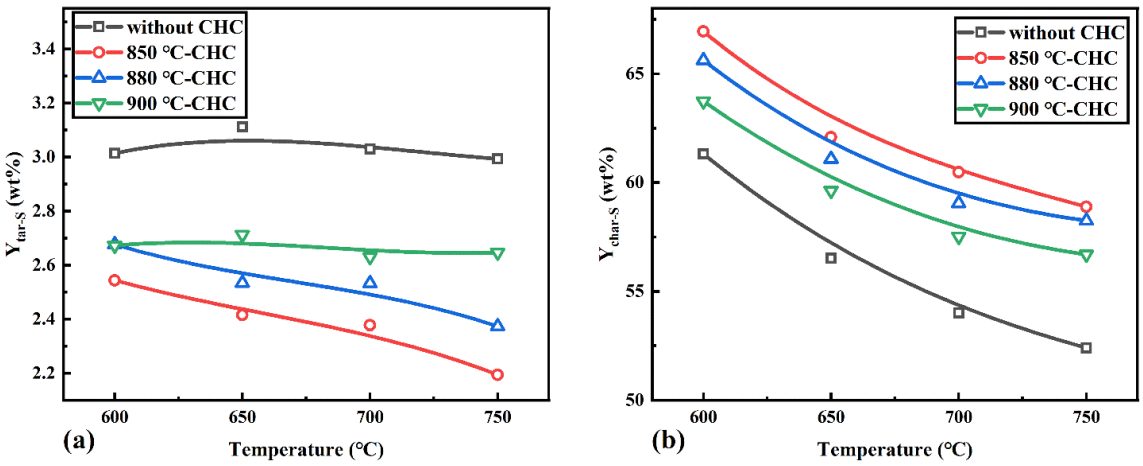

Figure 4. Effect of CHC production temperature on (a) $Y_{tar\text{-}S}$; (b) $Y_{char\text{-}S}$.

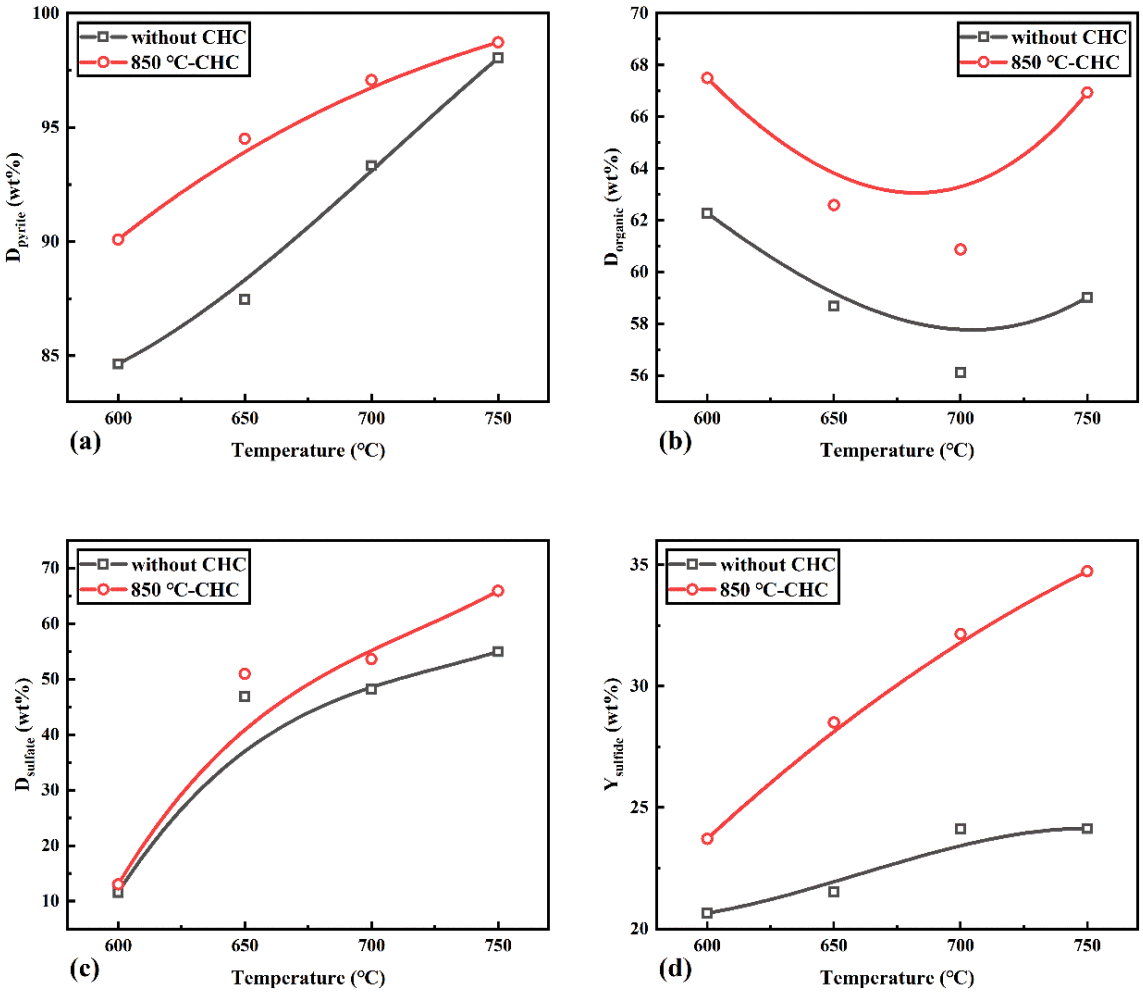

Figure 5. Variation of sulfur forms at different temperatures without and with 850 °C-CHC/coal = 3: (a) D_{pyrite}; (b) $D_{organic}$; (c) $D_{sulfate}$; (d) $Y_{sulfide}$.

Table 6. Carbon content of mixed-chars.

Temp. [°C]	Without CHC	850 °C-CHC/coal = 3
	C%, ad [wt %]	C%, ad [wt %]
600	75.47	73.04
650	76.76	74.28
700	73.00	68.10
750	71.12	65.06

COS in the form of CaS; secondly, CHC could promote the $D_{organic}$ and $D_{sulfate}$ to form sulfide.

This study is based on coal polygeneration technology, char and syngas are two main products. From the perspective of sulfur emission control, if the pyrolysis temperature is high and CHC/coal is relatively low, more sulfur will be released into the gas product, less sulfur will be residual in the char product, so the cost of desulfurization in the downstream processing of char utilization will become lower. Meanwhile, the choice of CHC with worse sulfur-fixation capacity causes less cost in the downstream processing of char utilization. According to the results obtained from this study, the combination of 750 °C pyrolysis temperature and 900 °C-CHC/coal = 3 is the best operating condition. On the contrary, when the operating condition leads to more sulfur released into gas, more desulfurization equipment should be arranged in the downstream processing of gas utilization. In practice, more factors should be taken into consideration at the same time beside sulfur emission, such as energy efficiency and feedstock property.

4 Conclusions

The sulfur conversion characteristics of XJRB during CHC pyrolysis were studied in a fluidized-bed reactor, and the effects of temperature, CHC/coal ,and CHC production temperature were investigated by determining the sulfur content of gas, tar, and mixed-char. The changes of sulfur forms in mixed-char were taken into consideration as well. Conclusions were obtained as follows:

- Y_{H_2S} and Y_{COS} rise with the increase of temperature, but the increment of Y_{H_2S} and Y_{COS} became smaller above 700 °C. Y_{CH_3SH} was relatively low, about 2 %, and decreased gradually when the temperature rose. $Y_{tar\text{-}S}$ was stable and unchanged with temperature. $Y_{char\text{-}S}$ was inhibited with the increasing temperature.
- The CHCs used in this study contained various minerals, such as CaO and FeS, among which CaO played the role of a H_2S and COS absorbent to fix them into CaS in mixed-char. Therefore, the Y_{H_2S} and Y_{COS} were reduced. However, the decrease of Y_{CH_3SH} was due to the catalytic effect of CHC on CH_3SH. Meanwhile, CHC was able to inhibit $Y_{tar\text{-}S}$. As the CHC/coal was raised, more CHC was introduced into the reaction system, being facilitated to inhibitory effect of CHC on Y_{H_2S} and $Y_{tar\text{-}S}$.
- The inhibitory effects of these three CHCs on Y_{H_2S}, Y_{COS}, and $Y_{tar\text{-}S}$ were ranked as follows: 850 °C-CHC > 880 °C-CHC > 900 °C-CHC. This was mainly attributed to the different microporous structures on their surfaces. The higher the CHC production temperature was, the less the microporous structures became, which was unfavorable for the reactions between the minerals and gaseous sulfur as well as the organic sulfur in tar. Because the Y_{CH_3SH} is low, the three CHCs showed no significant influence on it. In summary, 850 °C-CHC showed the best sulfur fixation performance, and the CHC/coal was chosen to be 3, considering the cost in practical application.
- Since the existence of CaO in CHC, $Y_{sulfide}$ elevated by the fixation effect of CaO on gaseous sulfur to form CaS residue in mixed-char. CHC showed a catalytic effect on the decomposition of pyrite, organic sulfur, and sulfate. Therefore, D_{pyrite}, $D_{organic}$, $D_{sulfate}$, and $Y_{sulfide}$ were all improved during pyrolysis process with CHC.

Data Availability Statement

The data that supports the findings of this study are available in the supplementary material of this article.

Supporting Information

Supporting Information for this article can be found under DOI: https://doi.org/10.1002/ceat.202300091.

Acknowledgment

This research was financially supported by the Fundamental Research Funds for the Central Universities (2022ZFJH004).

The authors have declared no conflict of interest.

Symbols used

C_{ar}	[vol %]	Ar concentration in gas
$C_{H_2S/COS/CH_3SH}$	[vol %]	concentration of H_2S, COS, or CH_3SH
D_i	[wt %]	decomposition rates of sulfur in *i*, where *i* represents one of sulfate, pyrite, and organic sulfur
M_{coal}	[g]	sample weight
$M_{tar}/M_{char}/M_{CHC}$	[g]	mass of tar, mixed-char, or CHC
$S_{i\text{-}char}/S_{i\text{-}CHC}/S_{i\text{-}coal}$	[wt %]	sulfur content of *i* in mixed-char, CHC, or coal
$S_{sulfide\text{-}char}/S_{sulfide\text{-}CHC}$	[wt %]	sulfur content of sulfide in mixed-char or CHC
S_T	[wt %]	total sulfur content
S_{tar}/S_{char}	[wt %]	sulfur content in tar or mixed-char
V_{Ar}	[L]	Ar volume consumed in 6 min
V_{gas}	[L]	total gas volume
V_m	[L mol^{-1}]	molar volume of gas
$Y_{H_2S/COS/CH_3SH}$	[wt %]	yield rates of sulfur in H_2S, COS, or CH_3SH
$Y_{sulfide}$	[wt %]	yield rate of sulfur in sulfide
$Y_{tar\text{-}S}/Y_{char\text{-}S}$	[wt %]	yield rates of sulfur in tar or mixed-char

Abbreviations

850 °C-CHC	CHC produced at 850 °C
BET	Brunauer-Emmett-Teller
CHC	char heat carrier
CHC/coal	CHC-to-coal mass ratio
COS	carbonyl sulfide
GC	gas chromatography
mixed-char	CHC and coal pyrolysis char
XJRB	Xin Jiang Run Bei coal
XRD	X-ray diffraction

References

[1] *Statistical Review of World Energy*, BP, London **2022**.
[2] J. Cen, M. Fang, Q. Wang, Z. Luo, K. Cen, *Chem. Ind. Eng. Prog.* **2011**, *30 (1)*, 88–94. DOI: https://doi.org/10.16085/j.issn.1000-6613.2011.01.012
[3] J. Saikia, P. Saikia, R. Boruah, B. K. Saikia, *Sci. Total Environ.* **2015**, *530–531*, 304–313. DOI: https://doi.org/10.1016/j.scitotenv.2015.05.109
[4] Y. Qi, W. Li, H. Chen, B. Li, *Fuel* **2004**, *83 (6)*, 705–712. DOI: https://doi.org/10.1016/j.fuel.2003.09.021
[5] Y. Qi, W. Li, H. Chen, B. Li, *Fuel* **2004**, *83 (16)*, 2189–2194. DOI: https://doi.org/10.1016/j.fuel.2004.06.009
[6] S. D. Feng, J. J. Fan, L. I. Ping, X. W. Ran, H. F. Yang, *Coal Eng.* **2018**, *50 (7)*, 133–136.
[7] Y. Duan, L. Duan, E. J. Anthony, C. Zhao, *Fuel* **2017**, *189*, 98–106. DOI: https://doi.org/10.1016/j.fuel.2016.10.080

[8] W. C. Xu, M. Kumagai, *Fuel* **2003**, *82 (3)*, 245–254. DOI: https://doi.org/10.1016/S0016-2361(02)00290-9

[9] Y. Qi, W. Li, H. Chen, B. Li, *J. China Univ. Min. Technol.* **2003**, *32 (2)*, 128–132. DOI: https://doi.org/10.3321/j.issn:1000-1964.2003.02.006

[10] F. Liu, B. Li, W. Li, Z. Bai, J. Yperman, *Fuel Process. Technol.* **2010**, *91 (11)*, 1486–1490. DOI: https://doi.org/10.1016/j.fuproc.2010.05.025

[11] M. Kozłowski, I. I. Maes, H. Wachowska, J. Yperman, D. v. Franco, J. Mullens, L. C. van Poucke, *Fuel* **1999**, *78 (7)*, 769–774. DOI: https://doi.org/10.1016/S0016-2361(98)00206-3

[12] H. Zhao, Z. Bai, J. Bai, Z. Guo, L. Kong, W. Li, *Fuel* **2015**, *148*, 145–151. DOI: https://doi.org/10.1016/j.fuel.2015.01.104

[13] M. A. Yuchuan, S. Yang, L. Chen, C. Zhao, S. Liu, D. U. Wenguang, J. Shangguan, *J. Taiyuan Univ. Technol.* **2019**, *50 (4)*, 453–459. DOI: https://doi.org/10.16355/j.cnki.issn1007-9432tyut.2019.04.007

[14] K. Sugawara, Y. Tozuka, T. Sugawara, Y. Nishiyama, *Fuel Process. Technol.* **1994**, *37 (1)*, 73–85. DOI: https://doi.org/10.1016/0378-3820(94)90007-8

[15] K. Miura, K. Mae, M. Shimada, H. Minami, *Energy Fuels* **2001**, *15 (3)*, 629–636. DOI: https://doi.org/10.1021/ef000185v

[16] Z. Shixue, Q. Jun, *Coal Convers.* **2000**, *23 (1)*, 44–46. DOI: https://doi.org/10.3969/j.issn.1004-4248.2000.01.009

[17] M. Guo, J. Bi, *Coal Convers.* **2016**, *39 (1)*, 26–30. DOI: https://doi.org/10.19726/j.cnki.ebcc.2016.01.006

[18] X. Jia, Q. Wang, K. Cen, L. Cheng, *Fuel* **2016**, *177*, 260–267. DOI: https://doi.org/10.1016/j.fuel.2016.03.013

[19] D. Pan, Q. Xuan, R. Zhang, B. Jicheng, *Coal Convers.* **2016**, *39 (3)*, 29–33. DOI: https://doi.org/10.3969/j.issn.1004-4248.2016.03.006

[20] D. Fu, X. Li, W. Li, J. Feng, *Fuel Process. Technol.* **2018**, *176*, 240–248. DOI: https://doi.org/10.1016/j.fuproc.2018.04.001

[21] Y. Zhang, M. Wang, Z. Qin, Y. Yang, C. Fu, L. Feng, L. Chang, *Fuel* **2013**, *103*, 915–922. DOI: https://doi.org/10.1016/j.fuel.2012.09.061

[22] X. Meng, J. Yang, Z. Ye, R. Chu, C. Wang, W. Li, X. Li, L. Feng, X. Jiang, *Fuel* **2022**, *308*, 121993. DOI: https://doi.org/10.1016/j.fuel.2021.121993

[23] N. Meng, D. Jiang, Y. Liu, Z. Gao, Y. Cao, J. Zhang, J. Gu, Y. Han, *Fuel* **2016**, *186*, 394–404. DOI: https://doi.org/10.1016/j.fuel.2016.08.097

[24] X. Jia, Q. Wang, L. Han, L. Cheng, M. Fang, Z. Luo, K. Cen, *J. Anal. Appl. Pyrolysis* **2017**, *124*, 319–326. DOI: https://doi.org/10.1016/j.jaap.2017.01.016

[25] G. Gryglewicz, S. Jasieńko, *Fuel* **1992**, *71 (11)*, 1225–1229. DOI: https://doi.org/10.1016/0016-2361(92)90047-R

[26] Q. Liu, H. Hu, Q. Zhou, S. Zhu, G. Chen, *Fuel Process. Technol.* **2004**, *85 (8–10)*, 863–871. DOI: https://doi.org/10.1016/j.fuproc.2003.11.031

[27] S. S. Chauk, R. Agnihotri, R. A. Jadhav, S. K. Misro, L. S. Fan, *AIChE J.* **2000**, *46 (6)*, 1157–1167. DOI: https://doi.org/10.1002/aic.690460608

[28] X. You, *Fuel Energy Abstr.* **2002**, *43 (4)*, 253. DOI: https://doi.org/10.1016/S0140-6701(02)86225-7

[29] R. Guan, W. Li, B. Li, *Fuel* **2003**, *82 (15–17)*, 1961–1966. DOI: https://doi.org/10.1016/s0016-2361(03)00188-1

[30] C. Sun, B. Li, C. E. Snape, *J. Fuel Chem. Technol.* **1997**, *25 (4)*, 358–362.

[31] S. Furfari, R. Cyprès, *Fuel* **1982**, *61 (5)*, 453–459. DOI: https://doi.org/10.1016/0016-2361(82)90071-0

[32] A. Attar, *Fuel* **1978**, *57 (4)*, 201–212. DOI: https://doi.org/10.1016/0016-2361(78)90117-5

[33] S. Yani, D. Zhang, *Fuel* **2010**, *89 (7)*, 1700–1708. DOI: https://doi.org/10.1016/j.fuel.2009.07.025

[34] J. Hou, Y. Ma, S. Li, W. Shang, *Carbon Resour. Convers.* **2018**, *1 (1)*, 86–93. DOI: https://doi.org/10.1016/j.crcon.2018.04.004

[35] F. Zhao, H. Zhao, R. Zhao, R. Liu, Y. Hu, *Chem. Eng.* **2006**, *34 (12)*, 31–35. DOI: https://doi.org/10.3969/j.issn.1005-9954.2006.12.009

